Title
Photochemical production of O3 in biomass burning plumes in the boundary layer over northern Australia

Journal
Geophysical Research Letters, 30(10)

ISSN
0094-8276

Authors
Takegawa, N
Kondo, Y
Ko, M
et al.

Publication Date
2003-05-15

DOI
10.1029/2003gl017017

Photochemical production of O_3 in biomass burning plumes in the boundary layer over northern Australia

N. Takegawa,[1] Y. Kondo,[1] M. Ko,[2] M. Koike,[3] K. Kita,[4] D. R. Blake,[5] W. Hu,[6] C. Scott,[7] S. Kawakami,[8] Y. Miyazaki,[1] J. Russell-Smith,[9] and T. Ogawa[8]

Received 30 January 2003; revised 26 March 2003; accepted 7 April 2003; published 17 May 2003.

[1] In situ aircraft measurements of ozone (O_3) and its precursors were made over northern Australia in August–September 1999 during the Biomass Burning and Lightning Experiment Phase B (BIBLE-B). A clear positive correlation of O_3 with carbon monoxide (CO) was found in biomass burning plumes in the boundary layer (<3 km). The $\Delta O_3/\Delta CO$ ratio (linear regression slope of O_3-CO correlation) is found to be 0.12 ppbv/ppbv, which is comparable to the ratio of 0.15 ppbv/ppbv observed at 0–4 km over the Amazon and Africa in previous studies. The net flux of O_3 exported from northern Australia during BIBLE-B is estimated to be 0.3 Gmol O_3/day. In the biomass burning region, large enhancements of O_3 were coincident with the locations of biomass burning hot spots, suggesting that major O_3 production occurred near fires (horizontal scale <50 km). *INDEX TERMS:* 0322 Atmospheric Composition and Structure: Constituent sources and sinks; 0365 Atmospheric Composition and Structure: Troposphere—composition and chemistry; 0368 Atmospheric Composition and Structure: Troposphere—constituent transport and chemistry. **Citation:** Takegawa, N., et al., Photochemical production of O_3 in biomass burning plumes in the boundary layer over northern Australia, *Geophys. Res. Lett.*, *30*(10), 1500, doi:10.1029/2003GL017017, 2003.

1. Introduction

[2] It has long been recognized that biomass burning is a major source of ozone (O_3) and its precursors in the tropics and subtropical regions [*Crutzen and Andreae*, 1990]. The NASA Transport and Atmospheric Chemistry Near the Equator Atlantic (TRACE-A) mission revealed that widespread biomass burning in the Amazon and southern Africa is the dominant source of O_3 and its precursors over the South Atlantic Basin [*Fishman et al.*, 1996]. Biomass burning activities in Indonesia and northern Australia are relatively weak as compared to those in the Amazon and southern Africa [*Galanter et al.*, 2000]. However, large enhancements of O_3 (>50 parts per billion by volume (ppbv)) were observed over Indonesia in October of 1994 and 1997 due to the extensive forest fires associated with El Niño events [*Fujiwara et al.*, 1999]. Biomass burning in northern Australia, commonly called "bushfire," takes place mainly during the austral dry season (from April/May to October/November) [*Russell-Smith et al.*, 2003]. The effects of biomass burning on O_3 and its precursors over northern Australia have not been fully evaluated because of the limited measurements of trace gases in this region [e.g., *Hurst et al.*, 1994]. The Biomass Burning and Lightning Experiment Phase B (BIBLE-B) campaign was conducted over Australia in August and September 1999 [*Kondo et al.*, 2002]. In this paper we investigate the photochemical production of O_3 in biomass burning plumes in the boundary layer over northern Australia during BIBLE-B.

2. Measurements

[3] In situ measurements of O_3, carbon monoxide (CO), nitric oxide (NO), non-methane hydrocarbons (NMHCs), and other species were made onboard the Gulfstream-II (G-II) aircraft. Details of the measurements are described by *Kondo et al.* [2002]. Figure 1 shows the flight tracks of the G-II during BIBLE-B, from August 31 to September 13, 1999 (Darwin local time). The locations of biomass burning hot spots during this period are shown in Figure 1. The hot spot data were obtained by the Advanced Very High Resolution Radiometer (AVHRR) onboard the National Oceanic and Atmospheric Administration satellite. In this analysis we use the data collected over the Arnhem Land region (11°–16°S, 129°–137°E) in the local afternoon (13:00–17:30 LT) at solar zenith angles of 25°–80°.

3. Results and Discussion

3.1. Correlation of O_3 and CO

[4] Details of the meteorological conditions and trace gas distributions over northern Australia during BIBLE-B are described by *Takegawa et al.* [2003]. Distinct inversion layers repeatedly appeared at 2–3 km over the Arnhem Land region, defining the top of the planetary boundary layer (PBL). The well-defined PBL was a strong barrier to the vertical transport of biomass burning emissions such as CO and nitrogen oxides (NO_x) in this region. Trajectory analysis showed that about 90% of the air masses sampled in the PBL over Arnhem Land were transported from the South Pacific under easterly flow conditions. This simple horizontal trans-

[1]Research Center for Advanced Science and Technology, University of Tokyo, Tokyo, Japan.
[2]NASA Langley Research Center, Hampton, Virginia, USA.
[3]Department of Earth and Planetary Science, University of Tokyo, Tokyo, Japan.
[4]Department of Environmental Science, Graduate School of Science, Ibaraki University, Ibaraki, Japan.
[5]Department of Chemistry, University of California, Irvine, California, USA.
[6]Department of Environmental Quality, Richmond, Virginia, USA.
[7]Atmospheric and Environmental Research Incorporated, Lexington, Massachusetts, USA.
[8]Earth Observation Research Center, National Space Development Agency of Japan, Tokyo, Japan.
[9]Bushfire Council of Northern Territory, Darwin, Australia.

0094-8276/03/2003GL017017

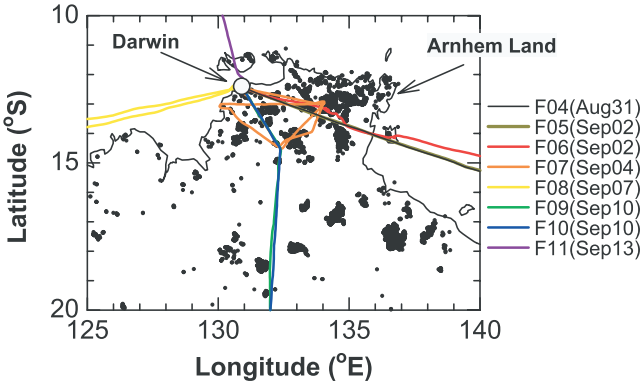

Figure 1. Flight tracks of the Gulfstream-II aircraft (colored lines) during the Biomass Burning and Lightning Experiment Phase B (BIBLE-B) campaign, from August 31 to September 13, 1999. The dates of the flights are shown in the legend. Dots show the locations of biomass burning hot spots observed by the Advanced Very High Resolution Radiometer (AVHRR) during the BIBLE-B period.

port pattern enabled us to determine the background levels of trace gases in this region. The background mixing ratios of O_3 and CO were estimated to be 36 ± 3 ppbv and 83 ± 6 ppbv, respectively, using air masses sampled upwind of Arnhem Land. Industrial pollution was a minor source of trace gases such as CO and NO_x in this region, and the enhancements of these gases above the background levels were dominated by biomass burning emissions.

[5] Correlation of O_3 with CO in the PBL (<3 km) over the Arnhem Land region is shown in Figure 2, together with the background mixing ratios of O_3 and CO. About 90% of the data shown in Figure 2 were obtained on September 2 (flight 6) and 4 (flight 7); the others were obtained on August 31 (flight 4) and September 10 (flight 10). A clear positive correlation of O_3 with CO was found in these air masses, indicating that O_3 was photochemically produced from its precursors that were emitted from biomass burning. The data obtained from different flights show a similar O_3-CO correlation. The best linear fit to the correlation is obtained when we restrict the data to CO < 250 ppbv. This range includes ~70% of the CO data (CO median = 190 ppbv). The $\Delta O_3/\Delta CO$ ratio is calculated to be 0.12 ± 0.04 ppbv/ppbv by a least squares fit. It is noted that the regression line passes through the uncertainty range of the background point, indicating that the estimated background mixing ratios are appropriate. The $\Delta O_3/\Delta CO$ ratio obtained in this study agrees with the ratio of 0.15 ppbv/ppbv observed at 0–4 km over the Amazon and Africa during TRACE-A [*Mauzerall et al.*, 1998] (Table 1). The agreement may reflect the similarity in the sampling conditions, such as latitude, season, altitude, NO_x/CO emission ratio, and plume age.

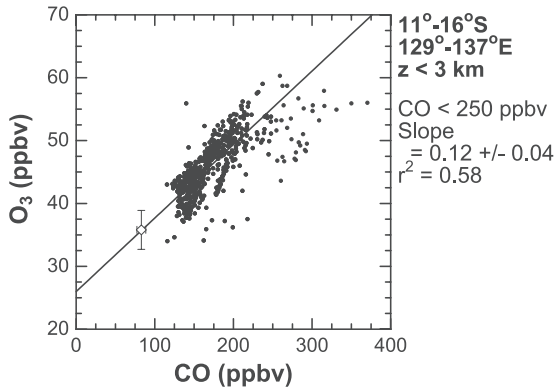

Figure 2. Correlation of O_3 with CO observed in the PBL (<3 km) over the Arnhem Land region (August 31, September 2, 4, and 10, 1999). The data are 10-s averages. The linear regression line (solid line) was determined by a least squares fit to the data at CO < 250 ppbv. The background mixing ratios of O_3 and CO and their uncertainties are shown as a diamond and bars, respectively.

Table 1. Comparison of $\Delta O_3/\Delta CO$ Ratios Observed During BIBLE-B and TRACE-A

	This study	*Mauzerall et al.* [1998]
Region	Australia (11°–16°S)	Amazon/Africa (7°–15°S)
Period	September 1999	September 1992
Altitude	1–3 km	0–4 km
ER (NO_x/CO)[a]	18 pptv/ppbv[b]	13 pptv/ppbv
Plume age	<~ 0.5 days[b]	~0.5 days
$\Delta O_3/\Delta CO$	0.12 ppbv/ppbv	0.15 ppbv/ppbv

[a]We assume that $\Delta NO_y/\Delta CO$ ratios observed in fresh biomass burning plumes were equal to the NO_x/CO emission ratio (*ER* (NO_x/CO)).
[b]*Takegawa et al.* [2003].

[6] We now estimate the net flux of O_3 exported from Arnhem Land in order to quantify the impact of biomass burning on the O_3 budget in this region. The $\Delta O_3/\Delta CO$ ratio is often referred to as the number of O_3 molecules produced per CO molecule emitted. Therefore, the CO emission amount multiplied by the $\Delta O_3/\Delta CO$ ratio gives the net flux of O_3 [*Parrish et al.*, 1993].

$$\text{Net flux of } O_3 = E(\text{CO}) \times \Delta O_3/\Delta CO, \quad (1)$$

where E(CO) denotes the daily emission of CO from the Arnhem Land region expressed in Gmol CO/day. *Chin et al.* [1994] pointed out that this simple approach could underestimate the O_3 flux when air masses were stagnated near the surface. This is because these air masses show a negative O_3-CO correlation in the absence of photochemistry. We consider that the equation (1) is applicable to the net flux of O_3 from Arnhem Land because of the simple transport pattern in this region (persistent easterly winds continuously flush the boundary layer). It should be noted that this study is the first to provide a quantitative estimate of the O_3 flux exported from northern Australia based on measurements. The E(CO) values were highly variable, ranging from ~0 to 8.8 Gmol CO/day (average 2.6 Gmol CO/day) between August 21 and September 14, 1999 [*Russell-Smith et al.*, 2003; *Shirai et al.*, 2003]. As a result, the net flux of O_3 exported from Arnhem Land during this period shows significant day-to-day variation, ranging from ~0 to 1 Gmol O_3/day (average 0.3 Gmol O_3/day). For comparison, *Wang et al.* [1998] reported that the photochemical production of O_3 in the Southern Hemispheric troposphere was ~80 Gmol O_3/day for an annual average.

3.2. O_3 Production Near Fires

[7] Figure 3 depicts the distribution of the O_3 mixing ratios observed at 1.7 km on September 2 (flight 6) and

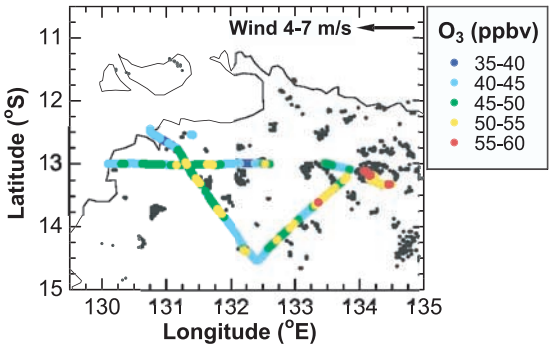

Figure 3. Horizontal distribution of O_3 mixing ratios observed at 1.7 km over the Arnhem Land region (September 2 and 4, 1999). Values are indicated by colored circles. Dots show the locations of hot spots observed by AVHRR on the days when the measurements were made. The wind speed (4–7 m/s) and direction (80°–125° from north) on those days are represented by an arrow.

4 (flight 7), 1999, together with the locations of biomass burning hot spots observed by AVHRR on September 2 and 4. According to the meteorological data provided by the European Centre for Medium-Range Weather Forecasts (ECMWF), the zonal wind speeds were 4–7 m/s and the wind directions were easterly/southeasterly (80°–125° from north) at 0–2 km over Arnhem Land on those days. It can be seen that the highest-O_3 areas were approximately coincident with the locations of hot spots. In order to quantify the horizontal scale more clearly, the O_3 mixing ratios are plotted as a function of horizontal downwind distance from the nearest hot spot (Figure 4). The uncertainty in determining the distance is estimated to be ~10 km, considering the difference among the distances from the nearest five hot spots. Some data points near hot spots show relatively low CO mixing ratios (100–150 ppbv). There are two possible explanations for this feature. One possibility is that biomass burning plumes were not well mixed with background air near fires, resulting in a large variability in the CO mixing ratios. The other possibility is the uncertainty in the locations of hot spots. The AVHRR hot spot data were taken at about

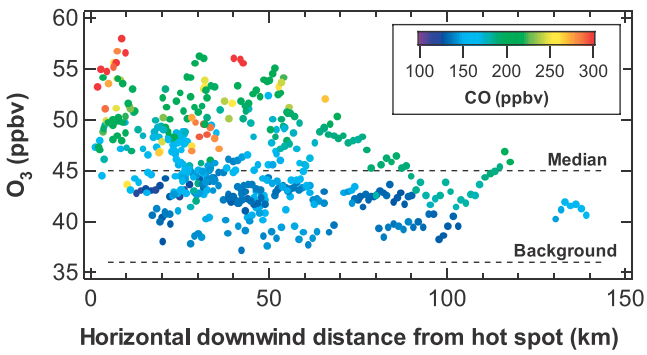

Figure 4. O_3 mixing ratio as a function of horizontal downwind distance from the nearest hot spot at 1.7 km over Arnhem Land (September 2 and 4, 1999). Data points are colored by CO mixing ratios. The background and median mixing ratios of O_3 (36 ppbv and 45 ppbv, respectively) are shown by dashed lines.

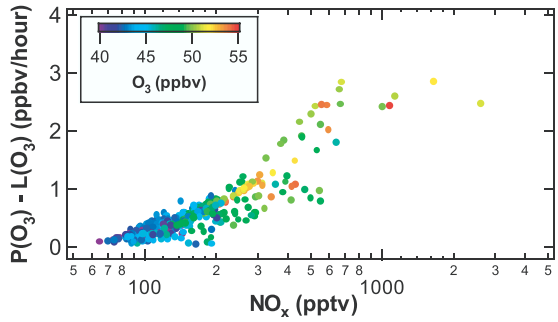

Figure 5. Instantaneous net O_3 production rate, $P(O_3) - L(O_3)$, as a function of NO_x mixing ratio at 1.7 km over Arnhem Land (September 2 and 4, 1999). Data points are colored by O_3 mixing ratios.

2:00–5:00 LT and 18:30–20:30 LT, while the aircraft measurements were made at 13:00–17:30 LT. Therefore, it is possible that the locations of fires during the aircraft measurements were slightly different from those of the hot spots observed by AVHRR. Despite these uncertainties, however, there is a clear tendency for the high-O_3 air masses to be found near hot spots, suggesting that major O_3 production occurred in the vicinity of fires. The air masses with O_3 enhancements of 10–20 ppbv above the background level (36 ppbv) were observed mostly at horizontal distances of <50 km. Considering the zonal wind speeds of 4–7 m/s, this result implies air mass ages of <3 hours and high O_3 production rates (>3 ppbv/hour) in these air masses.

[8] The photochemical box model described by *Ko et al.* [2002] was used to calculate the instantaneous O_3 production and loss rates in the observed air masses. The equations are given by

$$P(O_3) = (k_{NO+HO2}[HO_2] + k_{NO+RO2}[RO_2])[NO] \quad (2)$$

$$L(O_3) = k_{H2O+O1D}\left[O(^1D)\right][H_2O] + (k_{O_3+OH}[OH] + k_{O_3+HO2} \cdot [HO_2])[O_3], \quad (3)$$

where $P(O_3)$ and $L(O_3)$ are the instantaneous O_3 production and loss rates, respectively, RO_2 represents peroxy radicals (e.g., CH_3O_2), [X] is the number density of species X, and k_{X+Y} is the reaction rate coefficient for the X + Y reaction. The concentrations of O_3, NO, CO, methane (CH_4), and C_2-C_5 alkanes in the calculations were fixed at the observed values. The RO_2 concentrations were calculated using explicit oxidation schemes for CH_4 and ethane (C_2H_6) and using the *McKeen et al.* [1991] scheme for higher-order NMHCs. The photostationary-state nitrogen dioxide (NO_2) concentrations were also calculated using the box model. The sum of measured NO and calculated NO_2 is given as NO_x. Only data at solar zenith angles of <65° were used for the calculations. Figure 5 shows the $P(O_3) - L(O_3)$ values as a function of NO_x mixing ratio at 1.7 km over Arnhem Land. It clearly illustrates the strong dependence of $P(O_3) - L(O_3)$ on NO_x, which has been discussed by a number of investigators [e.g., *Jacob et al.*, 1996]. The model calculated $P(O_3) - L(O_3)$ shows a maximum value of ~3 ppbv/hour at NO_x >700 parts per trillion by volume (pptv). This value is smaller than the net O_3 production rates of >3 ppbv/hour derived from the observed O_3 enhancements and the

estimated air mass age. However, it is difficult to determine whether this is due to an underestimate of $P(O_3) - L(O_3)$ in the point model, considering that the number of data points at higher NO_x mixing ratios (>700 pptv) is limited.

[9] Although the above discussion is specific to the Arnhem Land region, the importance of accounting for O_3 production rates on a small horizontal scale has been discussed in previous studies. It has been pointed out that some regional/global chemical transport models (CTMs) may not appropriately reproduce the amount of O_3 production from biomass burning [*Chatfield and Delany*, 1990; *Poppe et al.*, 1998]. Even for a regional CTM with a horizontal resolution of 100 km × 100 km (1° in longitude × 1° in latitude), the model grid is typically much larger than the horizontal scale of each fire. O_3 production rates are often calculated using average concentrations of O_3 precursors in a relatively coarse model grid, by assuming that biomass burning plumes are instantaneously mixed in the grid. Because the O_3 production rates have a nonlinear dependence on NO_x, such an unrealistically fast dilution rate can lead to uncertainty in estimating the amount of O_3 produced. Indeed, *Poppe et al.* [1998] have shown that CTMs may either overestimate or underestimate the O_3 production amount, strongly depending on the rate of dilution.

4. Conclusions

[10] The $\Delta O_3/\Delta CO$ ratio was found to be 0.12 ppbv/ppbv in biomass burning plumes in the PBL over Arnhem Land during BIBLE-B. The net flux of O_3 exported from Arnhem Land during BIBLE-B was estimated to be 0.3 Gmol O_3/day, using the amount of CO emitted and the $\Delta O_3/\Delta CO$ ratio. The horizontal distribution of O_3 showed that the high-O_3 air masses were coincident with the locations of hot spots, suggesting that the major O_3 production occurred near fires (horizontal scale <50 km). This result implies the importance of O_3 production at a horizontal grid scale of smaller than 1° × 1°, which is generally difficult for regional/global models to resolve.

[11] **Acknowledgments.** The authors express sincere appreciation to D. D. Parrish for useful comments and discussions. The BIBLE-B mission was supported by the Earth Observation Research Center, National Space Development Agency of Japan (NASDA/EORC), and by the Japanese Ministry of Education, Culture, Sports, Science and Technology.

References

Chatfield, R. B., and A. C. Delany, Convection links biomass burning to increased tropical ozone, however, models will tend to over-predict O_3, *J. Geophys. Res.*, *95*, 18,473–18,488, 1990.

Chin, M., D. J. Jacob, J. W. Munger, D. D. Parrish, and B. G. Doddridge, Relationship of ozone and carbon monoxide over North America, *J. Geophys. Res.*, *99*, 14,565–14,573, 1994.

Crutzen, P. J., and M. O. Andreae, Biomass burning in the tropics: Impact on atmospheric chemistry and biogeochemical cycles, *Science*, *250*, 1669–1678, 1990.

Fishman, J., J. M. Hoell Jr., R. D. Bendura, R. J. McNeal, and V. W. J. H. Kirchhoff, NASA GTE TRACE A Experiment (September–October 1992): Overview, *J. Geophys. Res.*, *101*, 23,865–23,880, 1996.

Fujiwara, M., K. Kita, S. Kawakami, T. Ogawa, N. Komala, S. Saraspriya, and A. Suripto, Tropospheric ozone enhancements during the Indonesian forest fire events in 1994 and in 1997 as revealed by ground-based observations, *Geophys. Res. Lett.*, *26*, 2417–2420, 1999.

Galanter, M., H. Levy II, and G. R. Carmichael, Impacts of biomass burning on tropospheric CO, NO_x, and O_3, *J. Geophys. Res.*, *105*, 6633–6653, 2000.

Hurst, D. F., D. W. T. Griffith, and G. D. Cook, Trace gas emissions from biomass burning in tropical Australian savannas, *J. Geophys. Res.*, *99*, 16,441–16,456, 1994.

Jacob, D. J., et al., Origin of ozone and NO_x in the tropical troposphere: A photochemical analysis of aircraft observations over the South Atlantic basin, *J. Geophys. Res.*, *101*, 24,235–24,250, 1996.

Ko, M., W. Hu, J. M. Rodríguez, Y. Kondo, M. Koike, K. Kita, S. Kawakami, D. Blake, S. Liu, and T. Ogawa, Photochemical ozone budget during the BIBLE A and B campaign, *J. Geophys. Res.*, *107*(D3), 8404, doi:10.1029/2001JD000800, 2002.

Kondo, Y., M. Ko, M. Koike, S. Kawakami, and T. Ogawa, Preface to special section on Biomass Burning and Lightning Experiment (BIBLE), *J. Geophys. Res.*, *107*(D3), 8397, doi:10.1029/2002JD002401, 2002.

Mauzerall, D. L., J. A. Logan, D. J. Jacob, B. E. Anderson, D. R. Blake, J. D. Bradshaw, B. Heikes, G. W. Sachse, H. Singh, and B. Talbot, Photochemistry in biomass burning plumes and implications for tropospheric ozone over the tropical South Atlantic, *J. Geophys. Res.*, *103*, 8401–8423, 1998.

McKeen, S. A., E.-Y. Hsie, M. Trainer, R. Tallamraju, and S. C. Liu, A regional model study of the ozone budget in the eastern United States, *J. Geophys. Res.*, *96*, 10,809–10,845, 1991.

Parrish, D. D., J. S. Holloway, M. Trainer, P. C. Murphy, G. L. Forbes, and F. C. Fehsenfeld, Export of North American ozone pollution to the North Atlantic Ocean, *Science*, *259*, 1436–1439, 1993.

Poppe, D., R. Koppmann, and J. Rudolph, Ozone formation in biomass burning plumes: Influence of atmospheric dilution, *Geophys. Res. Lett.*, *25*, 3823–3826, 1998.

Russell-Smith, J., A. C. Edwards, and G. D. Cook, Reliability of biomass burning estimates from savanna fires; Biomass burning in northern Australia during the 1999 Biomass Burning and Lightning Experiment B field campaign, *J. Geophys. Res.*, *108*(D3), 8405, doi:10.1029/2001JD000787, 2003.

Shirai, T., et al., Emission estimates of selected volatile organic compounds from tropical savanna burning in northern Australia, *J. Geophys. Res.*, *108*(D3), 8406, doi:10.1029/2001JD000841, 2003.

Takegawa, N., et al., Removal of NO_x and NO_y in biomass burning plumes in the boundary layer over northern Australia, *J. Geophys. Res.*, *108*, doi:10.1029/2002JD002505, in press, 2003.

Wang, Y., J. A. Logan, and D. J. Jacob, Global simulation of tropospheric O_3 NO_x-hydrocarbon chemistry: 2. Model evaluation and global ozone budget, *J. Geophys. Res.*, *103*, 10,727–10,755, 1998.

D. R. Blake, Department of Chemistry, University of California, Irvine, CA 92697-2025, USA.

W. Hu, Department of Environmental Quality, 629 East Main Street, 8th Floor, Richmond, VA 23219, USA.

S. Kawakami and T. Ogawa, Earth Observation Research Center, National Space Development Agency of Japan, Tokyo, Japan.

K. Kita, Department of Environmental Sciences, Faculty of Science, Ibaraki University, 2-1-1 Bunkyo, Ibaraki 310-8512, Japan.

M. Ko, NASA Langley Research Center, Hampton, VA 23681-0001, USA.

M. Koike, Department of Earth and Planetary Science, Graduate School of Science, University of Tokyo, 7-3-1 Hongo, Bunkyo-ku, Tokyo 113-0033, Japan.

Y. Kondo, Y. Miyazaki, and N. Takegawa, Research Center for Advanced Science and Technology, University of Tokyo, 4-6-1 Komaba, Meguro, Tokyo 153-8904, Japan. (takegawa@atmos.rcast.u-tokyo.ac.jp)

J. Russell-Smith, Bushfire Council of the Northern Territory, Winnellie, NT 0821, Australia.

C. Scott Atmospheric and Environmental Research Incorporated, Lexington, MA 02421, USA.